The International Journal of Advanced Manufacturing Technology (2019) 101:2065–2081
https://doi.org/10.1007/s00170-018-3020-8

ORIGINAL ARTICLE

Hafnium and vanadium nitride multilayer coatings $[HfN/VN]_n$ deposited onto HSS cutting tools for dry turning of a low carbon steel: a tribological compatibility case study

J. H. Navarro-Devia[1] · C. Amaya[2] · J. C. Caicedo[3] · J. H. Martínez[1] · W. Aperador[1]

Received: 24 August 2018 / Accepted: 8 November 2018 / Published online: 27 November 2018

Abstract

This paper shows tribological compatibility enhancement in dry turning of a low carbon steel (AISI 1020) with High-speed steel cutting tools, due to physical vapor deposition (PVD) of hafnium and vanadium nitride multilayer coatings ($[HfN/VN]_n$), with different bilayer number system in each tool ($n = 1$, $n = 30$, $n = 50$, and $n = 80$). Tool wear mechanisms were assessed by means of scanning electron microscopy (SEM) and energy-dispersive X-ray spectroscopy (EDX) techniques, and surface integrity by roughness measurement and SEM inspection. Results show these multilayer coatings increase tool life up to 43%, and modify contact at tool/workpiece interface, as a function of bilayer number (n), due to their outstanding mechanical and tribological properties as a low coefficient of friction, high thermal conductivity, and high hardness; this produces a decrease of chip compression ratio, from 3.6 to 2.7, and workpiece roughness almost 1.6 μm lesser with the tool $[HfN/VN]_{80}$. Moreover, improvement of workpiece integrity includes its corrosion resistance, from a corrosion rate of 1.5 mmy, which decrease exponentially with higher bilayer number, to a corrosion rate lower than 0.1 mmy obtained with 80 bilayers, due to the change of chip morphology. Therefore, $[HfN/VN]_n$ coatings could enhance productivity and quality in an industrial manufacturing application, as these protective thin films increase tribological compatibility of tool/workpiece system.

Keywords Hard coating · Hafnium nitride · Vanadium nitride · Metal machining · Tool wear · Cutting tool · Multilayer · Tribology · Surface integrity

Highlights
- Hafnium and vanadium nitride multilayer coatings enhance tribological compatibility in dry turning of a low carbon steel with a coated high-speed steel cutting tool.
- Deposition of $[HfN/VN]_n$ coatings increase workpiece surface integrity and tool life.
- Workpiece corrosion and tool weight are also performance indicators.
- Tribological compatibility at workpiece/tool interface increases as a function of bilayer number.
- Chip compression ratio and tool wear decreased as functions of the $[HfN/VN]_n$ bilayer number.

✉ J. H. Navarro-Devia
u3900180@unimilitar.edu.co

✉ W. Aperador
g.ing.materiales@gmail.com

[1] School of Engineering, Universidad Militar Nueva Granada, Bogotá AA 110111, Colombia

[2] Development of Materials and Products Research Group, CDT-ASTIN SENA, Cali AA 760004, Colombia

[3] Tribology, Powder Metallurgy, and Processing of Solid Waste Research Group, Universidad del Valle, Cali AA 760032, Colombia

1 Introduction

One of the major problems in industries involving mass production processes is the impact of wear and cracks caused by friction between moving parts, use of worn tooling decreases the quality and quantity of the produced elements [1], causing supplementary costs in manufacturing processes, in addition to downtimes in the operations because of high frequency of stop of production, due to change of tool and reprocessing of the workpiece [2]. Cutting tools are a key consumable, and its consumptions is an indicator of manufacturing growth in a country economics, only in 2016 the total annual US consumption of cutting tools up to $2.042 billion dollars [3], and $2.195 billion dollars in 2017, due to a continuous rising machine tool orders [4, 5], an economical worldwide behavior throughout 2017 [6, 7]. Accordingly, researches to improve tool lifetime and workpiece quality are of extremely significant for industrial applications. Hard coatings deposition has been investigated and applied onto cutting tools to enhance

performance in industrial processes, due to the enhancement of the tribological characteristics of coated cutting tools, which improves tool lifetime and workpiece surface integrity, achieving a high degree of tribological compatibility within the cutting tool/workpiece system [8, 9]. Consequently, in 2007, it was estimated that coated cutting tools covered a 53% of the global market [10], and in 2016, 85% of all cemented carbide tools were coated [11].

Even though, hard coatings such as TiN, TiAlN, WC, ZrN, SiC, CrN, among others, have been studied and are deposited onto various cutting tools for machining of diverse materials [12–19]; there is a current interest in hafnium nitride (HfN) and vanadium nitride (VN) as an alternative or additional coating component, for a wide range of industrial applications, mainly by means of physical vapor deposition (PVD) or chemical vapor deposition (CVD) technique [20–29]. In the 1980s, HfN coatings were studied as a replacement of TiN coatings for gear cutting tools, due to this coating could offer a greater thermal barrier and hot hardness, but in that dates their production costs and times were so high related to TiN deposition processes [30]; thus, a more advanced technology were required for new PVD coatings on a base of transition metal nitride compounds [31]. However, due to the state-of-the-art equipment able nowadays, HfN monolayers, VN monolayers, and hafnium nitride-vanadium nitride multilayer ($[HfN/VN]_n$) coatings have been deposited onto a huge range of substrates, and their microstructure, chemical composition, morphology, topography, and layer thickness have been characterized; identifying properties as high hardness, high modulus of elasticity, and a critical load increase; which give an outstanding tribological behavior, with lesser friction coefficient; highlighting, performance of these thin films is better as multilayer and proportional to the bilayer number [32–41].

VN coating shows outstanding properties for tribological applications, as this nitride exhibits a low coefficient of friction (~0.65), increasing the lifetime of the tool on which it is deposited; on the other side, HfN has a hardness (~20 GPa) superior to most carbides and other nitrides such as TiN. In addition, HfN stoichiometry is one of the most stable compounds among transition metal mono-nitrides at high temperatures, making it an ideal candidate as a diffusion barrier [42]. Both nitrides (VN and HfN) are of interstitial-type, with metallic characteristics such as high thermal and electrical conductivity. Moreover, both materials have a high melting point, high hardness, and are chemically inert with properties of a refractory material [43, 44]. Therefore, HfN and VN coatings are an excellent alternative as a protective material for high-speed and high-temperature cutting tools.

These coatings have been deposited onto some cutting tools as thin films; C. Escobar et. al [45–47] characterized and studied HfN, VN, and [HfN/VN] thin films deposited onto tungsten carbide (WC) inserts, and their results showed flank wear decreases proportionally to bilayer number and suggest using [HfN/VN] multilayers as a protective coating for manufacturing processes. In addition, in previously published investigations, high-speed steel (HSS) cutting tools were coated with HfN, VN, and $[HfN/VN]_n$ thin films, and coating performance was evaluated by measurement of cutting temperature as a function of coating characteristics [48–53]. It was found their protective properties reduce cutting temperatures and thermal stress, which enhance workpiece surface roughness, due to $[HfN/VN]_n$ mechanical and tribological properties increase as function of bilayer number [45–48]; these studies output the potential of this multilayer coating for industrial application in manufacturing process, with higher wear resistance and tool lifetime.

In this work, the main purpose is to study the tribology compatibility of an HSS cutting tool/workpiece system in dry machining of AISI 1020 steel, with physical vapor deposition (PVD) of $[HfN/VN]_n$ multilayer coatings onto HSS tools. To achieve this, the resulting surface integrity of machined steel and tool wear were characterized, identifying a change in the manufacturing productivity and quality, as a function of $[HfN/VN]_n$ bilayer number.

2 Experimental details

2.1 Coating deposition

Firstly, for mechanical characterization purposes $[HfN/VN]_n$ multilayers were deposited onto silicon (100) substrates; successively, high-speed steel (HSS) cutting tool ASSAB 17 3/8″ × 3″ were coated for machining tests. These coating processes were realized using a multi-target r.f. magnetron sputtering system, with an r.f. source (13.56 MHz) for the applied negative voltage bias on each substrate, with 10-cm diameter targets of hafnium (Hf) and vanadium (V) with 99.9% purity; intermittently enclosed with a steel shutter. Previously, targets and substrates were sputter-cleaned during a 15-min period, an N_2-Ar gas-relation was injected into the chamber. The total measured thickness of the deposited HfN/VN multilayered coating was approximately 1.2 μm for all samples. The bilayer period thickness varied in function to the bilayer number from $n = 1$ to 80, producing bilayers period with thicknesses from 1200 to 15 nm, respectively [48]. Table 1 shows the deposition parameters applied to each cutting tool.

2.2 Coating mechanical properties characterization

The crystallographic structure characterized via X-ray diffraction (XRD), surface analysis by using a scanning electron microscope (SEM), chemical composition by X-ray photoelectron spectroscopy (XPS), coating thickness and coating

Table 1 $[HfN/VN]_n$ multilayer deposition parameters

Parameter	HfN	VN
Power density	4.5 W/cm	5.1 W/cm
N_2/Ar proportion	20–80%	20–80%
Gas flow	10 sccm	10 sccm
Working pressure	1.2×10^{-2} mbar	1.2×10^{-2} mbar
Vacuum pressure	2.5×10^{-5} mbar	2.5×10^{-5} mbar
Substrate temperature	250 °C	250 °C
Substrate-target distance	50 mm	50 mm
Deposition rate	385 nm/h	180 nm/h
R.f power	300 W	400 W
Polarization voltage	− 30 V	− 30 V

curvature determined by means of a profilometer, and multilayer numbers (n) measured by transmission electron microscopy (TEM) micrographs, have been reported previously for the same substrates and cutting tools used in this work [48]. In this research, the elasticity modulus (Er) and hardness (H) values were obtained by Oliver and Pharr's method [54, 55] in multilayered coatings deposited onto silicon (100) substrates, in nanoindentation test using an Ubi1-Hysitron device and a diamond Berkovich tip with a 10-mN maximum load [45, 47].

2.3 Machining test

With the aim of evaluating tribology compatibility of $[HfN/VN]_n$ multilayers in an industrial application, cylindrical turning in dry conditions of low-carbon steel rounded bars (AISI 1020), were carried out for the coated HSS ASSAB 17 cutting tool, and an uncoated tool as reference, using orthogonal array in a computer numerical controlled (CNC) lathe, PL6000M-DL6TM by Samsung machine tools with FANUC 0i-T control panel [48, 56, 57]. The chemical composition for the workpiece and the uncoated tool were provided by their manufacturers and are showed in Table 2.

Machining tests were performed in absence of lubrication (i.e., dry cutting) to expose $[HfN/VN]_n$ coatings under extreme tribological conditions and diverse wear mechanisms occurred due to higher cutting forces, higher cutting temperature, and no wet contact at the tool/workpiece interface [58, 59]. In addition, not only dry machining is considered as an environmentally friendly alternative, selection and effectiveness of the lubricant and the coating depend on cutting parameters, workpiece and tool materials, and coating composition, which modifies cutting forces and temperature, tool/chip contact length, surface roughness, tool life, and chip thickness [60–64].

In these tests, 5 different cutting tools were evaluated, one uncoated tool as the reference system, and 4 coated tools with different bilayer number system each ($n = 1$, $n = 30$, $n = 50$, and $n = 80$), 6 cutting tests per tool performed sequentially, for a total of 30 cutting tests. Testing conditions were, constants for each tests [48, 65], as follow: cutting speed (v) 125 mm/min, feed rate (f) 0.25 mm/rev, spindle speed (N) 500 rpm, surface speed of workpiece (V) 19.95 m/min, depth of cut (doc) 1 mm, steel bars diameter 12.7 mm (0.5 in), machined steel length per test 100 mm, cutting time per sample 48.3 s. Total cutting time per tool 290 s, cutting length (SCL) per sample 14.7 m, total cutting length per tool 88.2 m.

As workpiece surface integrity is influenced by tool wear and cutting performance [66, 67], the arithmetic average of the roughness profile (Ra) was selected as the variable of study, analyzed through a PCE-RT-1200 roughness tester, with a wavelength of 2.5 mm, palpation length of 5 mm, and resolution of 0.01 μm, taking 10 samples at each machined steel bar; hence, a total of 300 roughness measurements were performed [48, 56]. From SEM Jeol NeoScope JCM 5000, surfaces integrity of workpiece and worn tools were sequentially evaluated to observe coating influence. Tool wear was analyzed progressively, through optical microscopy, according to the tool-life testing international standard ISO 3685 [56, 68]; in addition, SEM and energy-dispersive X-ray spectroscopy (EDX) were used to investigate the morphology of the worn-cutting edges [8, 69]. Finally, to identify other possible changes in tribological compatibility (coating performance and surface integrity), the following evaluation methods were carried out: (I) tool mass of each cutting tool was measured with a resolution of 0.0001 g; (II) potentiodynamic-polarization test to identify corrosion rate of machined workpiece surfaces by the Tafel extrapolation method; (III) collecting chip samples during experimental tests followed by determining the average measurement of chip thickness to calculate chip compression ratio; and (IV) the chip underside was examined by means of SEM; all the above mentioned were performed to identify changes in the workpiece material removal process [70, 71].

Table 2 Chemical compositions and hardness for workpiece and uncoated cutting tool

Material wt%	C	Si	Mn	P	S	Cr	Mo	V	W	Hardness (Brinell)
AISI 1020	0.20	0.30	0.40	≤ 0.04	≤ 0.05	–	–	–	–	120
ASSAB 17	1.26	0.50	0.30	–	–	4.20	5.00	3.10	6.40	260

3 Results and discussion

3.1 Coating mechanical properties characterization

From nanoindentation tests, load-displacement depth curves for multilayer coatings are shown in Fig. 1, curves illustrate elastic and plastic deformation of each $[HfN/VN]_n$ coating.

Hardness and elastic modulus were estimated through Oliver and Pharr's method [54, 55]. The results are shown in Table 3, which illustrates a continuous increase in mechanical properties as a function of bilayer numbers, hardness and elastic modulus fluctuate from 25 up to 37 GPa, and from 264 up to 351 GPa, respectively. This offers a compressive stress relieving due to heterostructure effect, as bilayer period (Λ) is lower in [HfN/VN] thin films with a higher bilayer number [45, 47].

3.2 Workpiece superficial integrity analysis

3.2.1 Roughness surface analysis

Machined steel quality was quantified by measurement of the arithmetic roughness (Ra), as surface finish is influenced by tribological compatibility and interactions at the tool/workpiece interface, also roughness changes as tool wear increases and variations could indicate a failure or lifetime limit of the cutting tool [67, 72]. Figure 2 illustrates the average roughness of machined AISI 1020 steel bars by using each tool, and the error bars were obtained by standard deviation of the acquired data. It shows that workpiece have a lower roughness when is machined with coated tools, and for higher bilayer numbers ($n = 50$ and $n = 80$), roughness decreases up to 26.5% with lesser standard deviation; hence, this suggests a greater stability of the cutting process, due to HfN and VN coating characteristics, as has been reported by other studies [45, 49–52]. This roughness variation indicates a reduction in coefficient of friction and an enhancement of tribological compatibility by using $[HfN/VN]_n$ coatings to manufacture a smoother workpiece surface.

Table 3 Mechanical properties of $[HfN/VN]_n$ multilayer coatings

$[HfN/VN]_n$ bilayer number (n)	Hardness H (GPa) ± 0.1	Elastic modulus E_r (GPa) ± 1
$n = 1$	25.1	264
$n = 10$	29.6	292
$n = 30$	32.2	314
$n = 50$	35.6	319
$n = 80$	37.0	351

3.2.2 Optical and scanning electron microscopy surface analysis

Workpiece surfaces were evaluated by optical and scanning electron microscopy, and according to Ra values (Section 3.2.1), surface morphology changes as a function of bilayer number (n). Figures 3 and 4 display diverse workpiece surfaces, and it can be noticed a smoother and better surface was machined by increasing bilayer number.

The SEM micrographs of AISI 1020 steel machining surface after cutting test, at low (left figures) and high (right figures) magnifications, (Fig. 4a–j), expose abrasive wear and a huge amount of adhesive particles in the surfaces obtained with the uncoated tool (Fig. 4a, b), showing an abrasive mechanism such as cracks and variations of feed marks due to constant formation and break of BUE, which modifies nose radius and increase workpiece roughness. Instead, as $[HfN/VN]_n$ bilayer number upsurge more homogeneous surfaces are achieved (Fig. 4c–j), and feed grooves remain around 0.25 mm according to cutting parameters; in addition, more

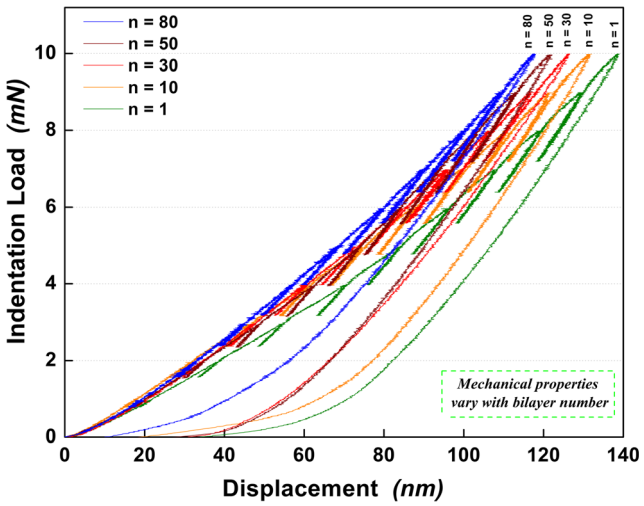

Fig. 1 Load-displacement depth curves for $[HfN/VN]_n$ multilayer coatings as function of bilayer number (n)

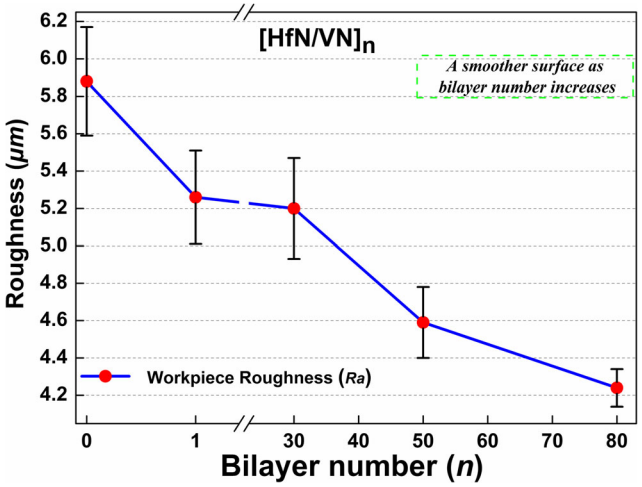

Fig. 2 Surface roughness (Ra) of machined steel with cutting tools coated with $[HfN/VN]_n$ multilayers, as a function of bilayers number

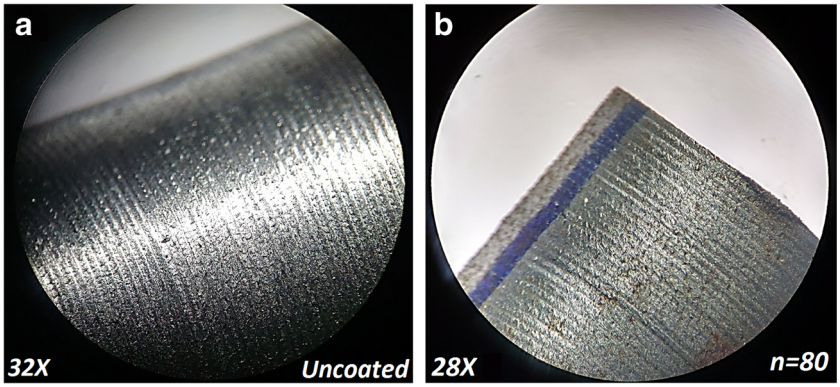

Fig. 3 Optical micrograph of machined surface morphology (steel bars) obtained with: **a** uncoated tool and **b** coated tool with bilayer number $[HfN/VN]_{80}$

frequent plastic deformation marks appear, from 0.25 mm reduce down to 0.16 mm proportional to $[HfN/VN]_n$ bilayer number, which suggests a change in chip formation due to a higher thermal stability and lower coefficient of friction at tool/chip interface, leading to have shorter chips (Section 3.3) and less rake tool wear (Section 3.4), enhancing workpiece surface finish.

3.3 Workpiece chip morphology and corrosion rate

3.3.1 Optical microscopy of chip morphology

The general chip formation were detected among the samples, and it was obtained chips of three form categories, according to ISO 3685—Table G.1 [68, 70], as shown in Fig. 5, i.e., washer-type helical chips (uncoated and $[HfN/VN]_1$), ribbon type chips ($[HfN/VN]_{30}$), and short spiral chips ($[HfN/VN]_{50}$ and $[HfN/VN]_{80}$).

This variation indicates a change in frictional behavior due to the coating properties, which influence cutting forces, shear stress, rake angle, and shear plane angle. Discontinuous chips are obtained at low cutting speeds in cutting tools with high thermal conductivity, leading to lower cutting temperatures, and continuous, tangled chips are at produced at higher average chip temperature, as a steady plastic flow of the workpiece material occurs on the tool face [73]. This shows that cutting tools with a high $[HfN/VN]_n$ bilayer number ($n = 50$ and $n = 80$) offer a more thermal stable process, with less friction, lower cutting temperature and energy dissipation onto chips, accordingly to the results of a previous work [48]. The transition from continuous to discontinuous chip formation is a gradual change of chip thickness ratio, due to an increase in shear angle and a decrease in cutting forces and shear strain within the primary shear zone [74, 75].

These chips were inspected in an optical microscope as a function of $[HfN/VN]_n$ bilayer number (Fig. 6) and by means of scanning electron microscopy (Fig. 7). It was identified that chip/tool interface area presents a smoother surface as bilayer number increases, with plastic deformation marks at steel machined with uncoated tool and $[HfN/VN]_1$ coated tool, due to higher thermal stability and a lower friction force in cutting tools with a high bilayer number, which reduce temperature at rake face as has been reported in other investigations [48, 53, 76].

3.3.2 SEM microscopy of chip underside

Chip underside was examined by SEM (Fig. 7), the chip underside produced by the uncoated tool shows the highest intensity of adhesion and abrasive marks. And chips obtained with a coated tool shown a decrease of chip thickness and adhesive particles adhered, due to a reduction of friction coefficient and heat dissipation at tool/chip interface as function of bilayer number, causing a lesser contact between the tool and the chip; and thus, the adhesion and built up edge (BUE) formation are reduced [76, 77]. In BUE formation in a continuous chip, particles adhere to the chip underside and path to the workpiece, raising poor surface finish, as was observed in Section 3.2, on the machined surface and accelerate wear on tool faces. So, discontinuous chip formation and chip underside indicate a lower wear at rake face and a higher tool life [67, 78, 79].

3.3.3 Chip compression ratio

The morphology results obtained in Sections 3.3.1 and 3.3.2, can be associated to changes in friction coefficient at the tool/chip interface due to increase in the bilayer number and $[HfN/VN]_n$ mechanical properties, this friction coefficient reduction causes a decreasing of chip compression ratio (CCR) [73]. CCR is the proportion between the deformed and the undeformed chip thickness, which represents the energy spent during plastic deformation, and wear mechanisms occurring during cutting, so higher CCR values indicate greater friction coefficients [69]. Hence, deformed chip thickness was measured 30 times, at every sample per cutting cycle of each tool, using a digital micrometer (Insize 3109), with 10-μm resolution, and the uncertainty of the carried out measurements of

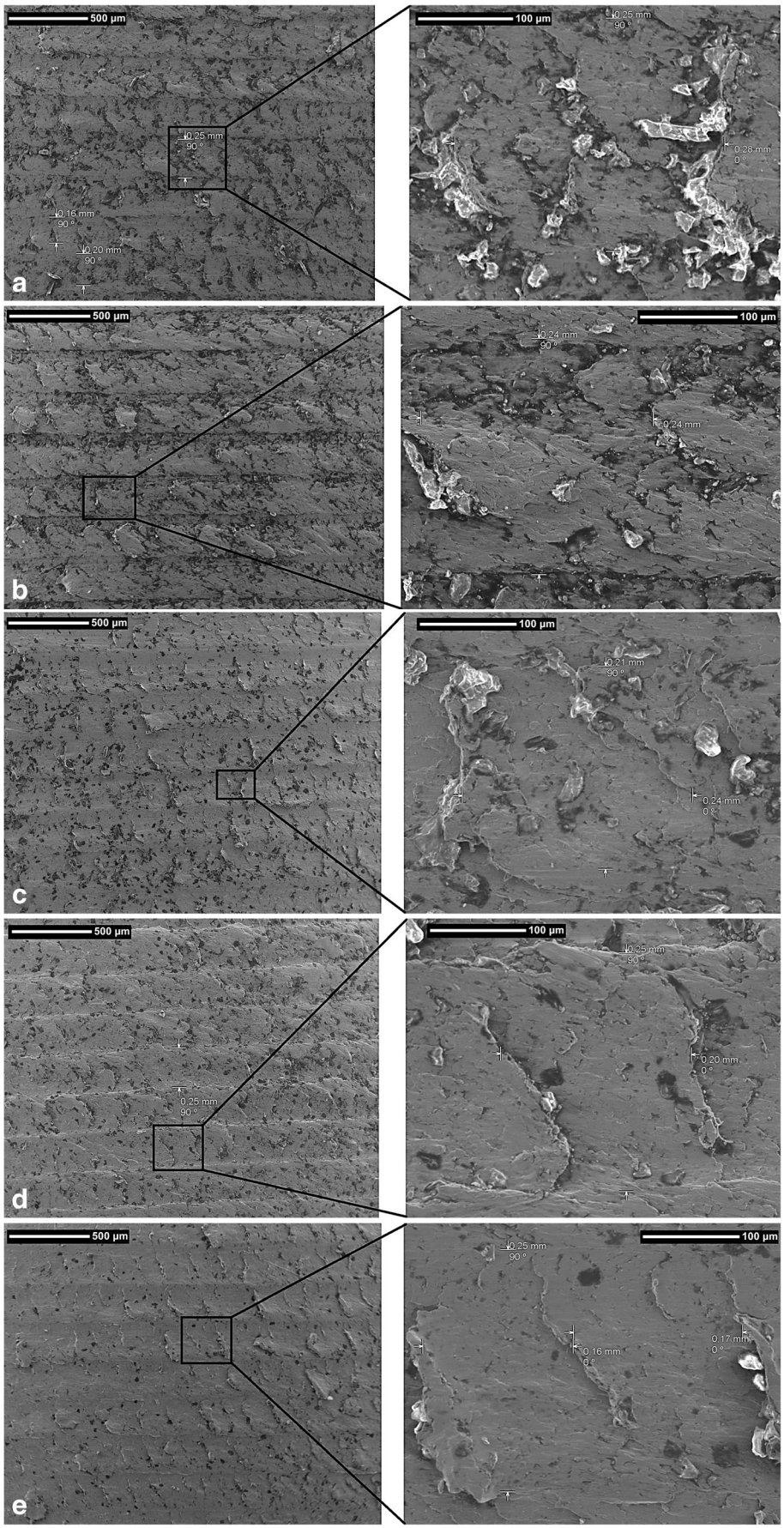

Fig. 4 SEM micrographs (50× and 300×) of surface morphology of machined steel with **a** uncoated tool, coated tool with bilayer number **b** tool/$[HfN/VN]_1$, **c** tool/$[HfN/VN]_{30}$, **d** tool/$[HfN/VN]_{50}$, and **e** tool/$[HfN/VN]_{80}$

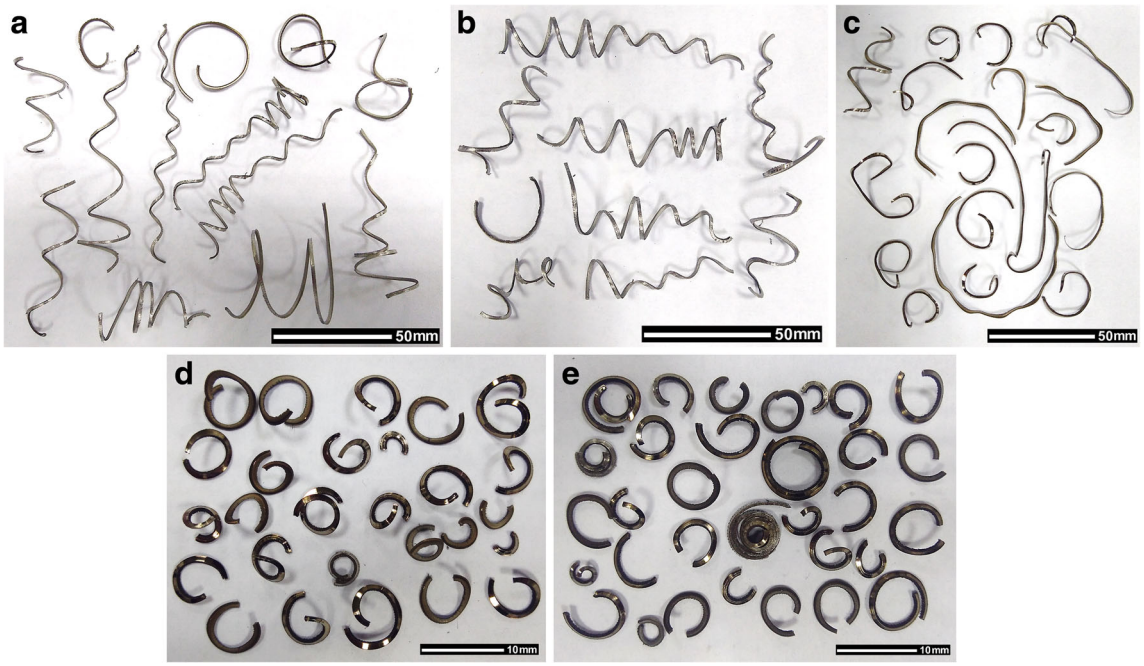

Fig. 5 AISI 1020 steel chips obtained from cutting test with: **a** uncoated tool, coated tool with bilayer number: **b** tool/[HfN/VN]$_1$, **c** tool/[HfN/VN]$_{30}$, **d** tool/[HfN/VN]$_{50}$, and **e** tool/[HfN/VN]$_{80}$

the chip thickness was around 10% [69]; thus, a total of 900 deformed chip thickness measurements were performed. Undeformed chip thicknesses and chip compression ratio were estimated according to Wright and Trent's methodology [80], which has been applied in previously published works [69, 75, 81, 82]. The chip compression ratio obtained for all cutting tools as a function of bilayer number is showed in Fig. 8.

Figure 8 reveals that cutting tools coated with [HfN/VN]$_n$ multilayers produce thinner chips, as CCR decreases when bilayer number is higher, due to the lower friction coefficient and outstanding tribological properties of this multilayer coating. In this sense, CCR decreases up to 25.5%, proportional to bilayer number, which creates lesser adhesion between the cutting tool and the workpiece material, thus decreasing wear rate (Section 3.4) [82].

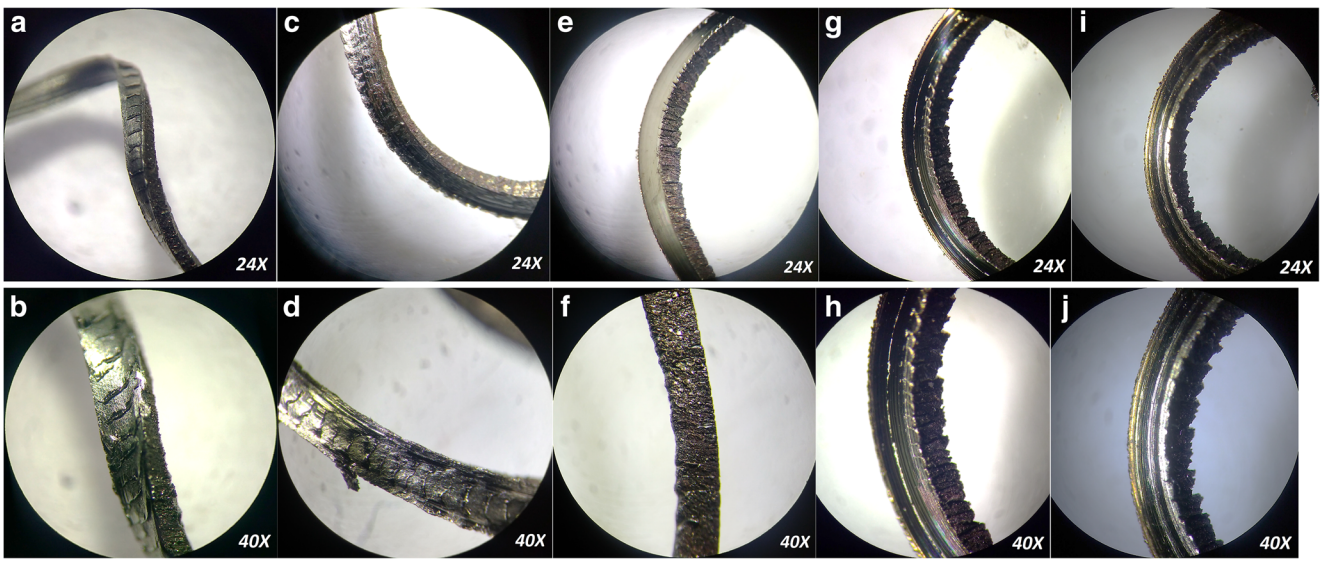

Fig. 6 Optical microscopy images (24× and × 40) of AISI 1020 steel chip obtained from cutting test with: **a**, **b** uncoated tool, coated tool with bilayer number **c**, **d** tool/[HfN/VN]$_1$, **e**, **f** tool/[HfN/VN]$_{30}$, **g**, **h** tool/[HfN/VN]$_{50}$, and **i**, **j** tool/[HfN/VN]$_{80}$

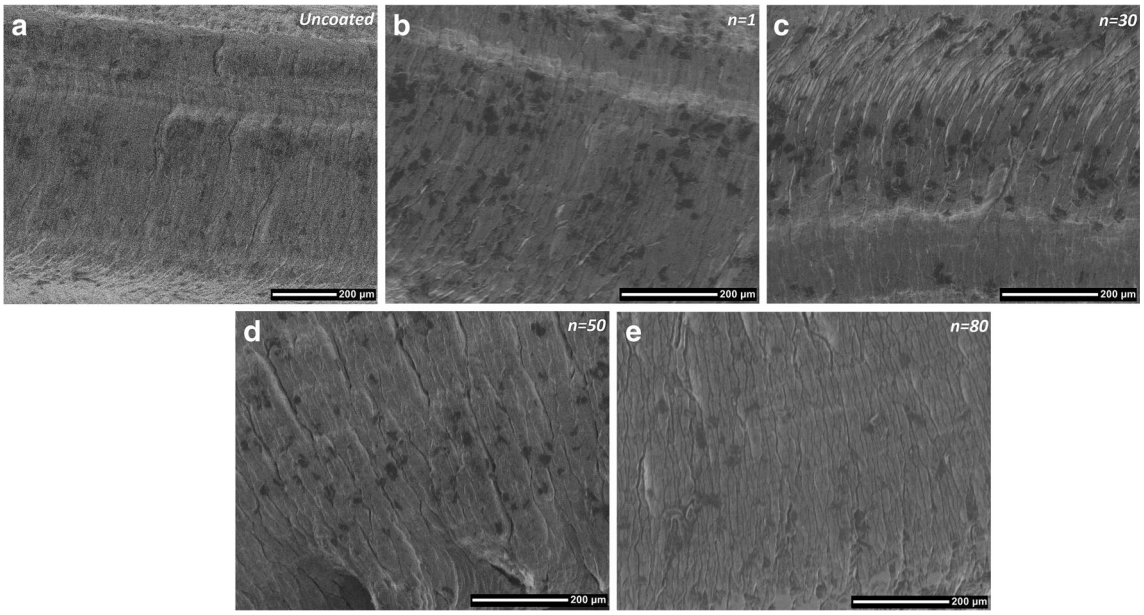

Fig. 7 SEM micrographs (150×) of produced AISI 1020 steel chip underside using diverse cutting tools: **a** uncoated tool, coated tool with bilayer number **b** tool/$[HfN/VN]_1$, **c** tool/$[HfN/VN]_{30}$, **d** tool/$[HfN/VN]_{50}$, and **e** tool/$[HfN/VN]_{80}$

3.3.4 Electrochemical measurements of the workpiece surface

Changes in workpiece surface (machined AISI 1020 steel bars) after machining process could include microstructural variations due to high-pressure zones and chemical compatibility at tool/workpiece interface, as shown above in SEM micrographs (Fig. 4—Section 3.2.2), which along with the cracks and irregular surfaces reduce fatigue and corrosion resistance of machined piece [67, 83]. Thus, potentiodynamic-polarization test was performed for workpieces, and the results reveal corrosion behavior and corrosion resistance change as function of the bilayer number (n). Figure 9 shows corrosion potential and current density (Tafel curves) on machined AISI 1020 steel by HSS cutting tools coated with $[HfN/VN]_n$ system, evidencing a corrosion resistance increasing when greater bilayer number was used.

The corresponding corrosion rates were obtained from Tafel extrapolation method [84], resulting in a remarkable difference among workpieces, (Fig. 10); steel bars machined with the reference uncoated tool will have a corrosion rate of around 1.5 mm per year (mmy), which reduces to 1.1 mmy in steel machined with $[HfN/VN]_n$ coated cutting tool with $n = 1$, and this rate decrease exponentially as bilayer number is higher; hence, steel machined with tool coated with $n = 80$ ($[HfN/VN]_{80}$) has a corrosion rate lower than 0.1 mmy; these

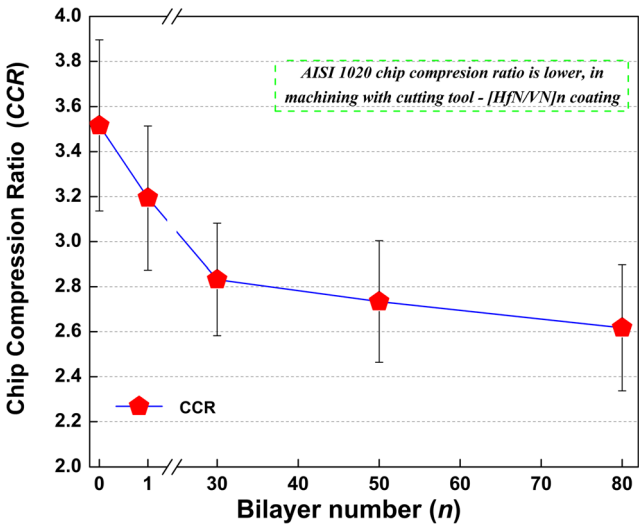

Fig. 8 Chip compression ratio, as a function of $[HfN/VN]_n$ bilayer number

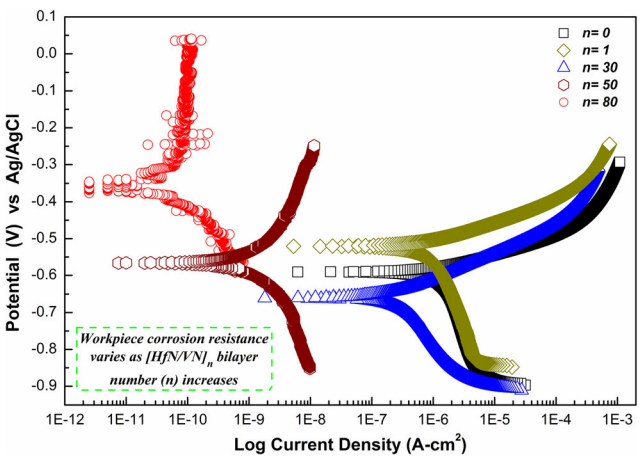

Fig. 9 Potentiodynamic-polarization curves of the machined AISI 1020 workpiece surfaces, by using an uncoated tool (HSS) and HSS tools, coated with $[HfN/VN]_n$ multilayers

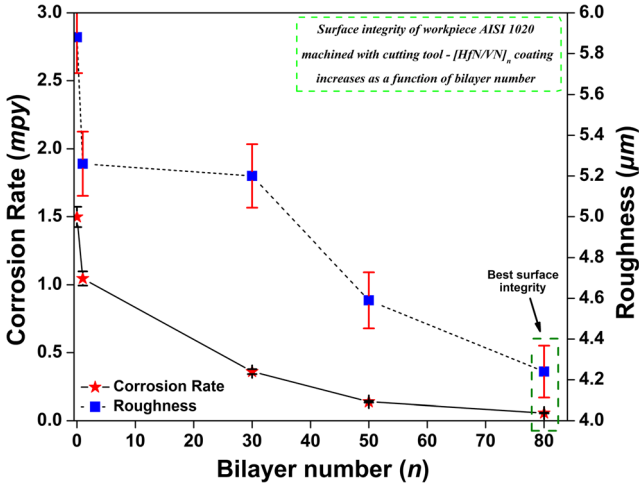

Fig. 10 Correlation between corrosion rate and roughness of machined AISI 1020 steel with cutting tools coated with $[HfN/VN]_n$, as a function of bilayer number (n)

results indicate that workpiece corrosion resistance is enhanced as superficial roughness decrease, both proportional to the bilayer number increasing in the cutting tools coated with $[HfN/VN]_n$ system.

To ratify corrosion rate results, a machined AISI 1020 steel obtained with uncoated HSS tool and a machined steel bar obtained with HSS tool coated $[HfN/VN]_{80}$ were stored for 1000 days, after this period these bars were evaluated by optical inspection (Fig. 11) and optical microscopy (Fig. 12). Workpiece machined with HSS tool coated $[HfN/VN]_{80}$ multilayers present a poorer oxide layer over the cutting zone compared to steel machined with uncoated HSS cutting tool; this indicates a higher corrosion resistance, accordingly to previous Tafel results (Fig. 9). These results shows that workpiece surface integrity are enhanced by using cutting tools coated with $[HfN/VN]_n$ multilayers, due to a reduction of corrosion rate and roughness proportional to bilayer number

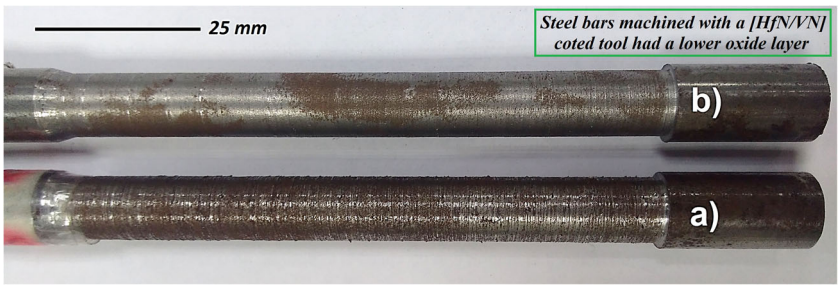

Fig. 11 Optical image of cylindrical machining bars surface, 1000 days after cutting test: **a** workpiece obtained with uncoated tool exhibits a high corrosion layer; and **b** workpiece obtained with a $[HfN/VN]_{80}$ coated tool, exhibits a low corrosion layer

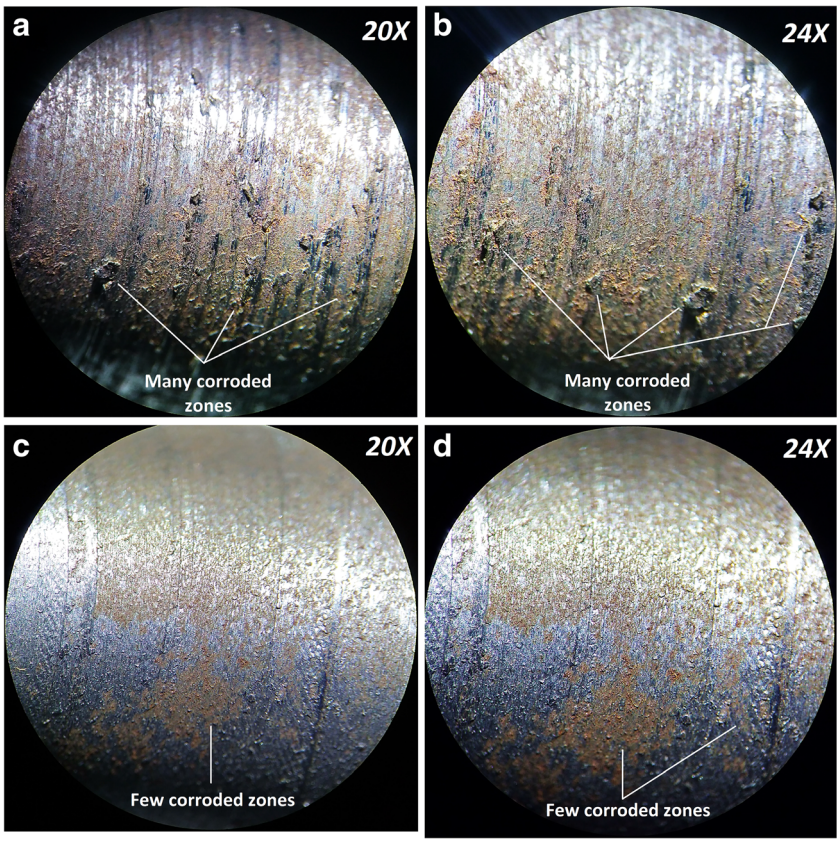

Fig. 12 Optical microscopy images of machined AISI 1020 steel bars, after 1000 days since cutting test with: **a**, **b** uncoated HSS tool and **c**, **d** HSS tool coated $[HfN/VN]_{80}$ multilayers

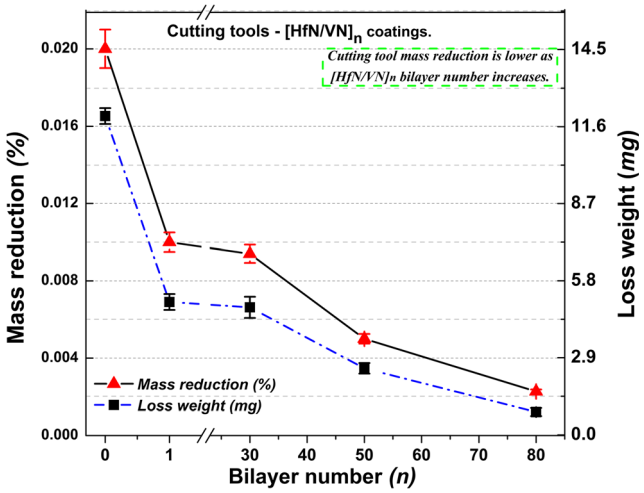

Fig. 13 Cutting tools mass reduction as a function of $[HfN/VN]_n$ bilayer number, after machining test

(Fig. 10), which is evidenced by a change in chip formation (Section 3.3.1), due to a change in the metal removal and tool performance by using like protective coating $[HfN/VN]_n$ multilayer thin films.

3.4 Tool life, wear resistant, and wear mechanisms

Wear mechanisms can be detected in relation to material removal, material surface, and mass transfer [67, 85, 86]; so, changes in tool weight can show wear resistance; hence, the weight of all tools was continuously measured through cutting tests. Figure 13 illustrates final mass reduction is lower as $[HfN/VN]_n$ bilayer number increases, which indicates a higher wear resistance due to the protective action of these coatings.

To quantify tool lifetime and identify wear mechanisms, the cutting tools (burins) were observed by optical microscopy to analyze the superficial changes (e.g., flank wear and rake wear) (Fig. 14). The flank wear of all cutting tools (ASSAB 17 burins) was small and similar due to the low cutting length (90 m) [87]. In contrast, in all the tools, it was observed notorious wear area at rake face, suggesting predominant wear is a combination of abrasion and diffusion wear [88], due to high temperature and contact within tool rake face and chip; it should be highlighted that built-up-edge (BUE) formation was visually identified only in the uncoated tool; hence, this reveals that $[HfN/VN]_n$ coatings contribute to decreasing adhesive wear due to their low friction coefficient, high hardness, and high-plastic deformation resistance; in rake face, worn areas were smaller with higher bilayer number ($[HfN/VN]_{80}$) (Fig. 15). It should be mentioned that no optical difference was identified between $[HfN/VN]_1$ and $[HfN/VN]_{30}$ coated tools.

Thus, is possible to observe that HfN/VN coatings minimize adhesive interaction at the tool/chip interface and abrasive contact [89]; in other words, these multilayers do not only enhance tool wear resistance; in addition, these coatings modify friction, wear, and chemical interactions of the tribo-couple [90], which indicates a better tribological compatibility has been achieved, and decrease wear area which exhibits a change in coloration, due to a reduction of temperature and stress in tool/chip interface, as a function of bilayer number.

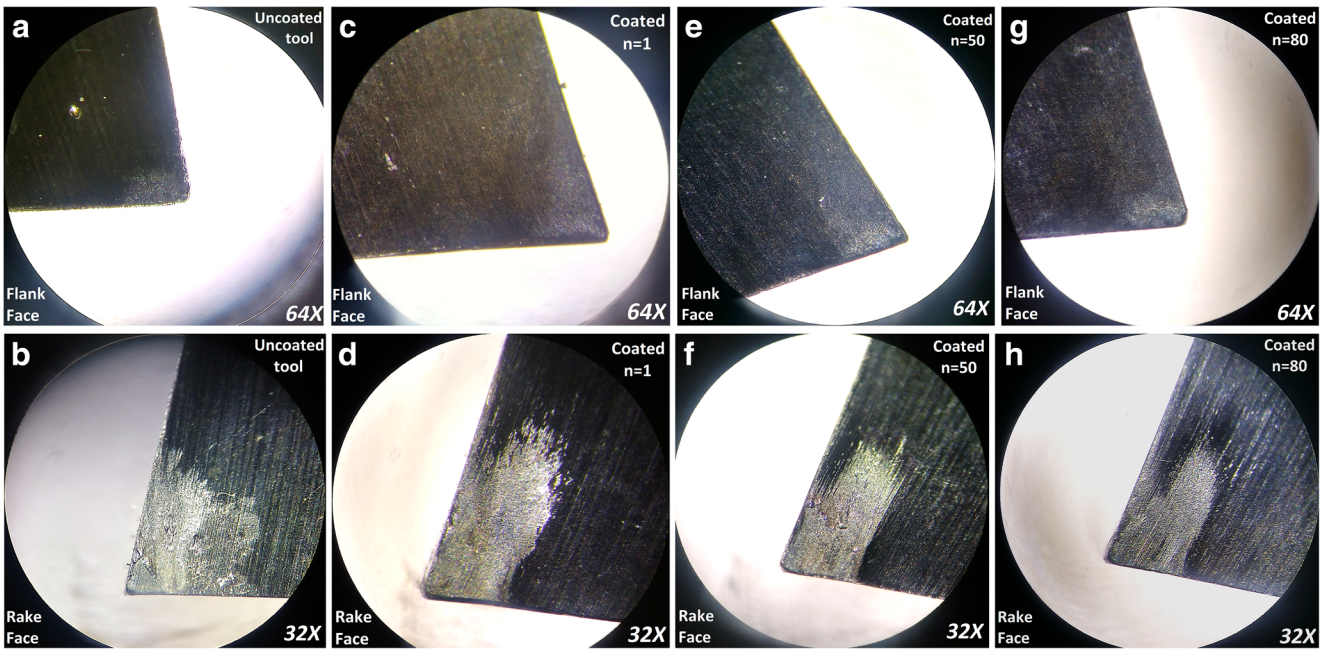

Fig. 14 Optical microscopy images of worn area for all cutting tools after machining test: **a**, **b** uncoated tool; cutting tool coated with **c**, **d** $[HfN/VN]_1$, **e**, **f** $[HfN/VN]_{50}$, **g**, **h** $[HfN/VN]_{80}$

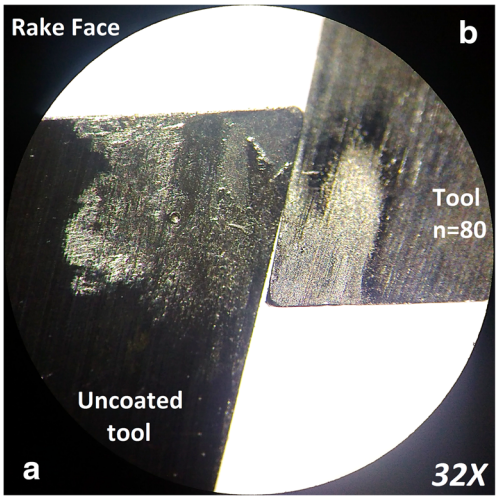

Fig. 15 Comparative image in optical microscopy (32×) of rake face after machining test: **a** uncoated tool and **b** cutting tool coated with $[HfN/VN]_{80}$

3.4.1 Wear curves

Figure 16 presents the flank wear (VB) curves for HSS cutting tools coated with $[HfN/VN]_n$ multilayers, VB analyses for HSS cutting tools were presented to 0, 30, and 90 m of cutting length. The coated tools with $[HfN/VN]_n$ exhibited lower VB compared to uncoated tool; wear was reduced as a function of reduced bilayer number. This behavior corresponds to excessive adhesive wear characteristic for this tribological system when the coating shows delaminating, which corresponds to reduced flank wear from 0.087 to 0.05 μm (88-m cutting length) for HSS uncoated to HSS coated deposited with $n = 80$ ($\Lambda = 15$ nm).

Figure 17 shows worn area growth in rake face, as crater wear is crucial for tool life limit according to the ISO standard, and could present different wear mechanism compared to flank wear [68, 87]. In the worn area, the higher wear rate occurred at

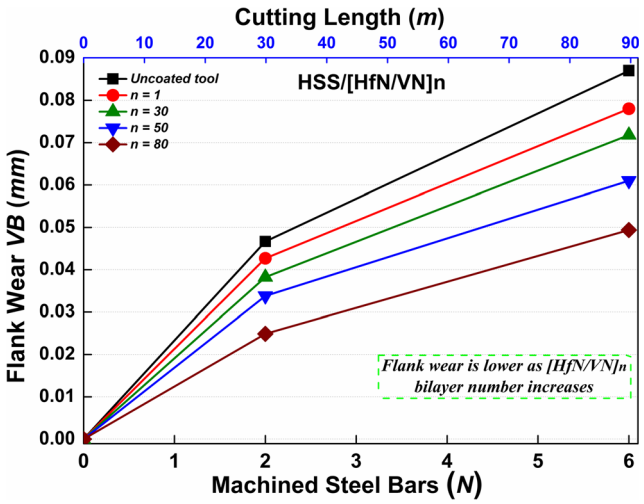

Fig. 16 Flank-wear curves of HSS cutting tools in dry turning of AISI 1020 steels

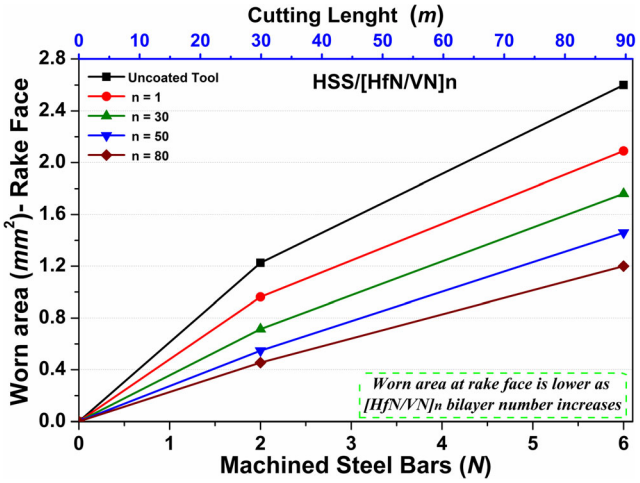

Fig. 17 Worn area at rake face of HSS cutting tools, throughout dry turning of AISI 1020 steels

uncoated tool, while coated tools experience gradual and steady wear throughout cutting test. In rake face, variation of worn area indicates a change in thermal behavior as a function of bilayer number. In the worn area, the wear shows a decrease with higher bilayer numbers, which indicates $[HfN/VN]_n$ coating increase tool life up to almost 45%. The good performance (45% enhanced tool life) for HSS cutting tools coated with high bilayer number presented on surface tool material can be attributed to high harness with relative high elastic modulus (Fig. 1). Low-friction coefficient produces a exceptional edge wear resistance, high strength, and resistance to deformation and depth of cut notch wear. These properties are adequate to endure the thermal and mechanical stresses produced in machining AISI 1020 steel, without suffering the inherent limitations of the PVD coatings (e.g., low adhesion and residual stresses on sharp edges that can induce coating delamination).

3.4.2 Wear mechanisms analyzed by SEM

Following, worn area (rake face) was inspected and analyzed by SEM, observing the wear mechanisms at SEM micrographs (Fig. 18), indicate adhesion was predominant wear mechanism in the uncoated tool; however, in coated tools, abrasive wear is dominant mechanism and the tool with $[HfN/VN]_1$ coating showed the biggest worn area. According to these micrographs, [HfN/VN] coatings reduce cutting temperature and cutting forces, due to their low-friction coefficient and higher thermal stability, which decrease adhesion and BUE formation [76]. Accordingly, abrasive marks reduce as a function of bilayer number, with an average width of 20 μm in the surface of $[HfN/VN]_{80}$-coated tool (Fig. 19), this indicates a more resistant capability against abrasive particles, due to low friction, hot hardness, and mechanical properties of these coatings. In addition, in the coated tools it was not identified surface damage or cracks formation (no critical failure).

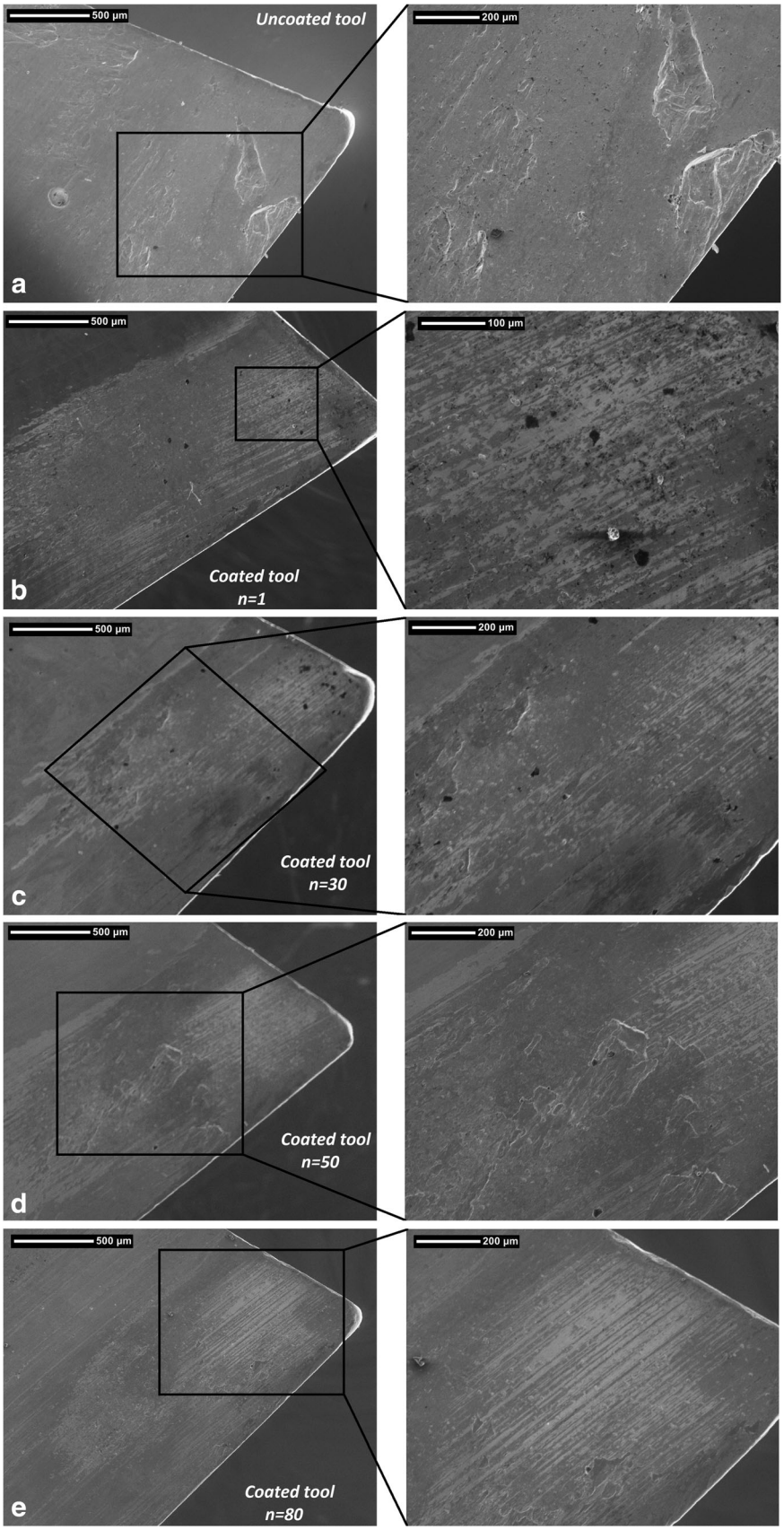

Fig. 18 SEM micrographs of the tool/chip contact area on the rake face exhibiting the worn area: **a** uncoated tool, coated **b** tool/$[[HfN/VN]_1$, **c** tool/$[HfN/VN]_{30}$, **d** tool/$[HfN/VN]_{50}$, and **e** tool/$[HfN/VN]_{80}$

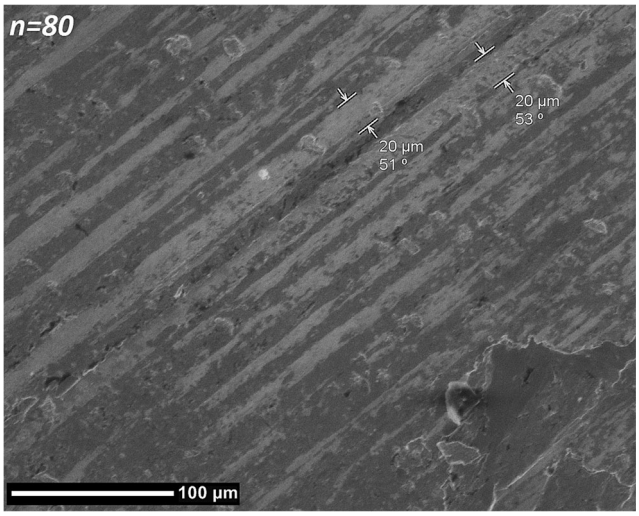

Fig. 19 SEM micrograph of abrasive marks at rake face of the [HfN/VN]$_{80}$-coated tool

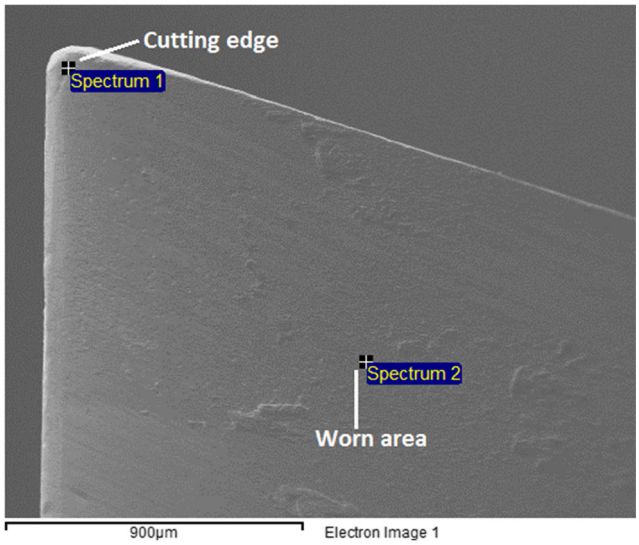

Fig. 20 EDX—spectrum on rake face after cutting test. **a** Spectrum 1 = cutting edge and **b** spectrum 2 = worn area

3.4.3 Chemical composition in the wear mechanism analyzed by EDX

Chemical composition analyzed by EDX was carried out to evaluate wear mechanisms in two dissimilar zones at rake face, associated to coating properties, such as cutting edge and worn area at cutting tools coated with [HfN/VN]$_n$ multilayer system after cutting test, shown in Fig. 20. Likewise, as a reference system, uncoated and [HfN/VN]$_1$-coated tools were also evaluated before cutting test. EDX results are shown in Table 4.

The results of EDX spectra on the rake face only identified nitrogen in the unused coated tool, which also presents the higher content of hafnium (Hf) and vanadium (V); this indicates that the coating is missing or damaged in the observed areas in all the tools after machining tests, including the BUE area; low content of Hf and V also suggests no formation of tribo-films (transferred or generated films), as these structures are usually formed in high-speed or high-temperature cutting process [69, 91]. In the cutting edge surface, carbon content decrease as a function of bilayer number, due to a reduction of BUE formation and workpiece material adhered, accomplish a better adhesive wear resistant, according to SEM micrographs (Section 3.4.2).

In this sense, the tribological pair was compound by HfN/VN bilayer and AISI 1020 bar; therefore, interaction of the cutting tool/workpiece system can produce iron (Fe) particles (debris), so the (Fe) was the major element present in the tribological surface, due to the Fe comes out from steel substrate and steel bars. Taking in account last discussion, the workpiece and uncoated tool major element (Fe) can be an indicator to quantify wear intensity [87], where the higher percentages were found in the [HfN/VN]$_{50}$ and the [HfN/VN]$_{80}$-coated tools, and indicates a lower wear concentration is required, in cutting tools uncoated and coated with low bilayer number, to increase wear area and accelerate crater

Table 4 Chemical composition of worn surface in [HfN/VN]$_n$ coated tools

Sample		Content (atomic percentage)													
		C K	Cr K	Mn K	Fe K	Co K	Mo L	W M	O K	Cl K	N K	Si K	Hf L	V K	Total
[HfN/VN]1	Edge	29.12	2.96	–	43.01	6.26	0.8	0.74	10.29	–	–	–	5.43	1.39	100
	Worn area	29.45	1.96	0.38	50.17	3.74	0.81	1.18	8.79	0.24	–	–	0.4	2.88	
[HfN/VN]30	Edge	26.94	0.99	–	27.66	1.93	–	–	19.22	–	–	–	11.7	11.56	
	Worn area	23.42	–	0.52	59.37	–	–	–	16.32	–	–	0.37	–	–	
[HfN/VN]50	Edge	19.67	3.44	0.35	64.13	8.03	1.11	1.35	–	–	–	–	–	1.92	
	Worn area	11.53	0.18	0.64	77.43	–	–	–	9.97	–	–	0.25	–	–	
[HfN/VN]80	Edge	10.6	3.24	0.52	58.41	7.61	0.88	0.94	16.41	–	–	–	–	1.39	
	Worn area	27.2	–	0.57	61.94	–	–	–	9.95	–	–	0.34	–	–	
Reference system	Uncoated	21.78	3.81	0.33	59.42	9.21	1.27	1.62	–	–	–	–	–	2.56	
	Coated	8.47	–	–	6.4	0.66	–	–	23.03	–	16.84	–	19.46	25.14	

Table 5 Percentage change in the results, as a function of $[HfN/VN]_n$ bilayer number

$[HfN/VN]_n$ bilayer number	Workpiece roughness—reduction (%)	Chip compression rate—reduction (%)	Corrosion rate—reduction (%)	Tool mass loss—reduction (%)	Tool life—increase (%)	Wear area at rake face—reduction (%)
$n = 1$	10.5	9.2	30.2	50.0	10.3	19.6
$n = 30$	11.6	19.5	76.0	53.0	18.0	41.5
$n = 50$	21.9	22.2	90.8	75.0	29.9	43.8
$n = 80$	27.9	25.6	96.2	90.0	43.2	53.8

wear formation, according to the intensity of the abrasive wear identified above (Sections 3.4.1 and 3.4.2).

3.5 Tribological compatibility enhancement—coating performance

The results show that wear performance improvement is greater on the rake face than at flank face, which suggest $[HfN/VN]_n$ coatings reduce the tool temperature and adhesive damage, and once heat generation is reduced the major characteristics of machining rose simultaneously [8], as it was observed in a previous research about cutting temperature in a turning process with these multilayer coatings [48]. In addition, the reduction of wear rate in both tool faces is also due to lower coefficient of friction and the increase of hardness, elastic modulus, and thermal strength on the coated tools, which has a major impact against abrasive wear [71]. All coated cutting tools had alike predominant wear mechanisms: adhesive wear on the flank surface and abrasive wear on the rake surface, with a significant reduction of built-up edge formation.

Therefore, tribological compatibility is higher as $[HfN/VN]_n$ multilayer coatings minimize adhesive interaction at the tool/chip interface and increase resistant to abrasion contact [89]; in other words, these multilayers do not only enhance superficial wear resistance of the cutting tools; in addition, these coatings modify friction, wear, and thermochemical interactions of the tribo-pair [90], increasing workpiece surface integrity as function of bilayer number (n), which indicates a better tribological compatibility has been achieved, with a reduction of stress in tool/chip interface; and thus, achieve a lower surface roughness and higher corrosion resistant of workpiece, with an enhancement of tool life by means of a slower material reduction and thinner chip formation throughout the machining process; all these results are summarized in Table 5.

4 Conclusions

A tribological compatibility enhancement among a HSS cutting tool and a low carbon workpiece, throughout dry machining, was achieved by deposition of $[HfN/VN]_n$ multilayers coatings, which increase wear resistance in the flank face and rake face, due to their physical-chemical properties, reduce friction coefficient and enhance tool life.

An improvement of workpiece superficial integrity is achieved by using a cutting tool with $[HfN/VN]_n$ multilayer coatings, as they reduce coefficient of friction and increase thermal stability proportional to bilayer number, which causes a formation of discontinuous chips, lower surface roughness, and an increase of corrosion resistance in machined low carbon steel.

The characterization of wear mechanisms, chip formation, and surface integrity of the machined part were performed after aggressive dry machining conditions using cutting tools with hard PVD coatings, by means of SEM; where in all the evaluated parameters, it was obtained a growing enhancement as a function of bilayer number. Furthermore, corrosion resistance of machined material is raised due to lesser formation of superficial damage and cracks throughout the cutting process, which is influenced by the properties of the deposited coating.

$[HfN/VN]_n$ multilayer thin films as protective coating deposited onto a HSS cutting tool, increase the tribological compatibility in a turning process of a low carbon steel, increasing tool lifetime and machined workpiece integrity, due to their outstanding tribological properties, which do not only raise wear resistant of the cutting tool; they have a low coefficient of friction so cutting forces are reduced, along with their behavior as a thermal barrier, modify interactions of the tribo-pair. Consequently, chip compression ratio is lower with a thinner chip formation as adhesive contact between tool and workpiece is lesser reducing forces and temperature in at interface, producing a smoother surface in the machined steel, that improve workpiece integrity by means of rising corrosion resistance. Therefore, $[HfN/VN]_n$ multilayer coatings modify interactions of the tribo-pair, increasing workpiece surface integrity and tool lifetime, as a function of bilayer number (n), which suggests this coating could be applied to enhance the manufacturing productivity and quality in an industrial case.

Authors' contribution and interest All authors contribute to discussion of the results. For experimental tests, the contributions of each author were the following: J.H. Navarro-Devia: machining tests, roughness measurement, workpiece

inspection, chip morphology evaluation, and tool wear mechanism analysis. *C. Amaya*: coatings deposition. J.C. Caicedo: coatings characterization, tool wear mechanisms analysis. J. H. Martínez: machining tests, workpiece, and chips and tool wear inspection. W. Aperador: coatings characterization, workpiece corrosion, wear inspection, and research project supervision. All authors contribute to writing this article and have approved the final version.

Research data Data will be made available on request.

Funding This research was supported and funded by "Vicerrectoría de Investigaciones de la Universidad Militar Nueva Granada" project no. ING-2630 (validity 2018) and by Colciencias under call "Convocatoria 761—Jóvenes Investigadores e Innovadores 2016."

Compliance with ethical standards

Conflict of interest The authors declare that they have no conflict of interest.

Publisher's Note Springer Nature remains neutral with regard to jurisdictional claims in published maps and institutional affiliations.

References

1. Zhang Z, Li X, Almandoz E, Fuentes GG, Dong H (2017) Sliding friction and wear behaviour of Titanium-Zirconium-Molybdenum (TZM) alloy against Al 2 O 3 and Si 3 N 4 balls under several environments and temperatures. Tribol Int 110:348–357. https://doi.org/10.1016/j.triboint.2016.10.049
2. Gachot C, Rosenkranz A, Hsu SM, Costa HL (2017) A critical assessment of surface texturing for friction and wear improvement. Wear 372–373:21–41. https://doi.org/10.1016/j.wear.2016.11.020
3. Brooks R (2017) US cutting tool consumption fell 4.3% in 2016. Am. Mach. Wkly
4. Brooks R (2018) US cutting tool consumption rose 8.3% for 2017. Am. Mach. Wkly
5. Brooks R (2017) Rising machine tool orders indicate continuing expansion. Am. Mach. Wkly
6. Brooks R (2017) Machine tool demand still strong, expanding. Am. Mach. Wkly
7. Brooks R (2017) Latest machine tool orders show manufacturing still expanding. Am. Mach. Wkly
8. Veldhuis SC, Dosbaeva GK, Yamamoto K (2009) Tribological compatibility and improvement of machining productivity and surface integrity. Tribol Int 42:1004–1010. https://doi.org/10.1016/j.triboint.2009.02.004
9. Vereschaka A, Aksenenko A, Sitnikov N, Migranov M, Shevchenko S, Sotova C, Batako A, Andreev N (2018) Effect of adhesion and tribological properties of modified composite nanostructured multi-layer nitride coatings on WC-Co tools life. Tribol Int 128:313–327. https://doi.org/10.1016/j.triboint.2018.07.039
10. Davies MA, Ueda T, M'Saoubi R et al (2007) On the measurement of temperature in material removal processes. CIRP Ann - Manuf Technol 56:581–604. https://doi.org/10.1016/j.cirp.2007.10.009
11. Bobzin K (2017) High-performance coatings for cutting tools. CIRP J Manuf Sci Technol 18:1–9. https://doi.org/10.1016/j.cirpj.2016.11.004
12. Paiva J, Fox-Rabinovich G, Locks Junior E, Stolf P, Seid Ahmed Y, Matos Martins M, Bork C, Veldhuis S (2018) Tribological and wear performance of nanocomposite PVD hard coatings deposited on aluminum die casting tool. Materials (Basel) 11:358. https://doi.org/10.3390/ma11030358
13. Yamamoto K, Abdoos M, Paiva J, Stolf P, Beake B, Rawal S, Fox-Rabinovich G, Veldhuis S (2018) Cutting performance of low stress thick TiAlN PVD coatings during machining of compacted graphite cast iron (CGI). Coatings 8:38. https://doi.org/10.3390/coatings8010038
14. Vereschaka A, Kataeva E, Sitnikov N, Aksenenko A, Oganyan G, Sotova C (2018) Influence of thickness of multilayered nanostructured coatings Ti-TiN-(TiCrAl) N and Zr-ZrN-(ZrCrNbAl) N on tool life of metal cutting tools at various cutting speeds. Coatings 8:44. https://doi.org/10.3390/coatings8010044
15. Sui X, Li G, Jiang C, Wang K, Zhang Y, Hao J, Wang Q (2018) Improved toughness of layered architecture TiAlN/CrN coatings for titanium high speed cutting. Ceram Int 44:5629–5635. https://doi.org/10.1016/j.ceramint.2017.12.210
16. Kong Y, Tian X, Gong C, Chu PK (2018) Enhancement of toughness and wear resistance by CrN/CrCN multilayered coatings for wood processing. Surf Coatings Technol 344:204–213. https://doi.org/10.1016/j.surfcoat.2018.03.027
17. Pogrebnjak AD, Ivashchenko VI, Skrynskyy PL, Bondar OV, Konarski P, Załęski K, Jurga S, Coy E (2018) Experimental and theoretical studies of the physicochemical and mechanical properties of multi-layered TiN/SiC films: temperature effects on the nanocomposite structure. Compos Part B Eng 142:85–94. https://doi.org/10.1016/j.compositesb.2018.01.004
18. Maksakova O, Simoẽs S, Pogrebnjak A, Bondar O, Kravchenko Y, Beresnev V, Erdybaeva N (2018) The influence of deposition conditions and bilayer thickness on physical-mechanical properties of CA-PVD multilayer ZrN/CrN coatings. Mater Charact 140:189–196. https://doi.org/10.1016/j.matchar.2018.03.048
19. Li H-Y, He H-B, Han W-Q, Yang J, Gu T, Li YM, Lyu SK (2015) A study on cutting and tribology performances of TiN and TiAlN coated tools. Int J Precis Eng Manuf 16:781–786. https://doi.org/10.1007/s12541-015-0103-4
20. Chang Y-Y, Chang H, Jhao L-J, Chuang C-C (2018) Tribological and mechanical properties of multilayered TiVN/TiSiN coatings synthesized by cathodic arc evaporation. Surf Coatings Technol 350:1071–1079. https://doi.org/10.1016/j.surfcoat.2018.02.040
21. Tillmann W, Lopes Dias NF, Stangier D (2018) Effect of Hf on the microstructure, mechanical properties, and oxidation behavior of sputtered CrAlN films. Vacuum 154:208–213. https://doi.org/10.1016/j.vacuum.2018.05.015
22. Shypylenko A, Lisovenko M, Belovol K, et al (2017) Effect of Hf addition and deposition condition on the structure and properties of the Ti-Hf-Si-N coatings. In: 2017 IEEE 7th international conference nanomaterials: application & properties (NAP). IEEE, p 02NTF32-1-02NTF32-5
23. Stanciu I, Predoana L, Preda S, Calderon-Moreno JM, Stoica M, Anastasescu M, Gartner M, Zaharescu M (2017) Synthesis method and substrate influence on TiO 2 films doped with low vanadium content. Mater Sci Semicond Process 68:118–127. https://doi.org/10.1016/j.mssp.2017.06.021
24. Chang S-Y, Chen B-J, Hsiao Y-T, Wang DS, Chen TS, Leu MS, Lai HJ (2018) Preparation and nanoscopic plastic deformation of toughened Al-Cu-Fe-based quasicrystal/vanadium multilayered coatings. Mater Chem Phys 213:277–284. https://doi.org/10.1016/j.matchemphys.2018.04.045
25. Piedrahita WF, Aperador W, Caicedo JC, Prieto P (2017) Evolution of physical properties in hafnium carbonitride thin films. J Alloys Compd 690:485–496. https://doi.org/10.1016/j.jallcom.2016.08.109
26. Song J, Cao L, Jiang L, Liang G, Gao J, Li D, Wang S, Lv M (2018) Effect of HfN, HfC and HfB 2 additives on phase transformation,

microstructure and mechanical properties of ZrO 2-based ceramics. Ceram Int 44:5371–5377. https://doi.org/10.1016/j.ceramint.2017.12.164
27. Contreras E, Galindez Y, Rodas MA, Bejarano G, Gómez MA (2017) CrVN/TiN nanoscale multilayer coatings deposited by DC unbalanced magnetron sputtering. Surf Coatings Technol 332:214–222. https://doi.org/10.1016/j.surfcoat.2017.07.086
28. Chang Y-Y, Weng S-Y, Chen C-H, Fu F-X (2017) High temperature oxidation and cutting performance of AlCrN, TiVN and multilayered AlCrN/TiVN hard coatings. Surf Coatings Technol 332:494–503. https://doi.org/10.1016/j.surfcoat.2017.06.080
29. HongYu Y (2014) Hafnium: chemical characteristics, production and applications., 1st ed. Nova
30. Kelly PW (1984) Advantages of titanium nitride coated gear tools. Gear Technol 1:12–23 ,48
31. Fox-Rabinovich GS, Kovalev AI, Afanasyev SN (1996) Characteristic features of wear in tools made of high-speed steels with surface engineered coatings I. Wear characteristics of surface engineered high-speed steel cutting tools. Wear 201:38–44. https://doi.org/10.1016/S0043-1648(96)07203-1
32. Staia MH, Bhat DG, Puchi-Cabrera ES, Bost J (2006) Characterization of chemical vapor deposited HfN multilayer coatings on cemented carbide cutting tools. Wear 261:540–548. https://doi.org/10.1016/j.wear.2006.01.005
33. Mora Parada MJ (2014) Propiedades Tribocorrosivas De Monocapas De HfN, VN Y Multicapas [HfN/VN] n depositadas sobre acero AISI 4140. **UPTC**
34. Escobar C, Villarreal M, Caicedo JC et al (2013) Mechanical and tribological behavior of VN and HfN films deposited via reactive magnetron sputtering. Surf Rev Lett 20:1350040. https://doi.org/10.1142/S0218625X13500406
35. Escobar CA, Caicedo JC, Aperador W (2014) Corrosion resistant surface for vanadium nitride and hafnium nitride layers as function of grain size. J Phys Chem Solids 75:23–30. https://doi.org/10.1016/j.jpcs.2013.07.024
36. Escobar C, Villarreal M, Caicedo JC, Aperador W, Caicedo HH, Prieto P (2013) Diagnostic of corrosion–erosion evolution for [Hf-Nitrides/V-Nitrides] n structures. Thin Solid Films 545:194–199. https://doi.org/10.1016/j.tsf.2013.07.081
37. Escobar C, Villarreal M, Caicedo JC, Aperador W, Prieto P (2014) Mechanical properties of steel surfaces coated with HfN/VN superlattices. J Mater Eng Perform 23:3963–3974. https://doi.org/10.1007/s11665-014-1194-2
38. Escobar C, Caicedo JC, Caicedo HH, Mozafari M (2014) Design of hard surfaces with metal (Hf/V) nitride multinanolayers. J Superhard Mater 36:366–380. https://doi.org/10.3103/S1063457614060021
39. Escobar C, Caicedo JC, Aperador W et al (2013) Improve on corrosion resistant surface for AISI 4140 steel coated with VN and HfN single layer films. Int J Electrochem Sci 8:7591–7607
40. Escobar C, Villarreal M, Caicedo JC, Aperador W, Prieto P (2013) Novel performance in physical and corrosion resistance HfN/VN coating system. Surf Coatings Technol 221:182–190. https://doi.org/10.1016/j.surfcoat.2013.02.002
41. Caicedo JC, Escobar C, Aperador W, Caicedo HH, Prieto P (2015) Heterostructures design for Hf-Nitride/V-Nitride system. J Phys Chem Solids 87:87–94. https://doi.org/10.1016/j.jpcs.2015.08.004
42. Arranz A (2004) Synthesis of hafnium nitride films by 0.5–5 keV nitrogen implantation of metallic Hf: an X-ray photoelectron spectroscopy and factor analysis study. Surf Sci 563:1–12. https://doi.org/10.1016/j.susc.2004.06.162
43. Pierson HO (1996) Handbook of refractory carbides & nitrides: properties, characteristics, and applications. Noyes Publications, New Jersey
44. Storms EK (1972) Phases relationships and electrical properties of refractory carbides and nitrides. Solid State Chem 10
45. Escobar C, Caicedo HH, Caicedo JC (2016) Hafnium and vanadium nitride heterostrutures applied to machining devices. Int J Adv Manuf Technol 82:369–378. https://doi.org/10.1007/s00170-015-7345-2
46. Escobar C, Villarreal Montenegro MS, Caicedo JC et al (2014) Tribological and wear behavior of HfN/VN nanomultilayer coated cutting tools. Ing e Investig 34:22–28. https://doi.org/10.15446/ing.investig.v34n1.41101
47. Escobar Claros CA, Villarreal Montenegro MS (2011) Obtención y Caracterización De Recubrimientos De HfN, VN Y HfN/VN Para Su Aplicación En La Industria Metalmecánica. Universidad del Valle
48. Navarro-Devia JH, Amaya C, Caicedo JC, Aperador W (2017) Performance evaluation of HSS cutting tool coated with hafnium and vanadium nitride multilayers, by temperature measurement and surface inspection, on machining AISI 1020 steel. Surf Coatings Technol 332:484–493. https://doi.org/10.1016/j.surfcoat.2017.08.074
49. Navarro-Devia JH, Aperador WA, Delgado A (2016) Performance evaluation of monolayer hafnium nitride coated tool for cutting | Evaluación del Desempeño de Buriles con Recubrimiento Monocapas de Nitruro de Hafnio en el Proceso de Mecanizado. Inf Tecnol 27:. https://doi.org/10.4067/S0718-07642016000100014
50. Navarro-Devia JH, Aperador WA, Delgado A (2017) Machining on AISI 1020 using monolayer vanadium nitride coated tool bit // Mecanizado de Acero AISI1020, Utilizando Buriles con Recubrimiento Monocapa de Nitruro de Vanadio. Inf tecnológica 28:77–86. https://doi.org/10.4067/S0718-07642017000100008
51. Guzman Durán PA, Navarro-Devia JH, Aperador W (2016) Machining with cutting tool coated with monolayer of HfN. TECCIENCIA (21):1–6. https://doi.org/10.18180/tecciencia.2016.21.1
52. Navarro-Devia JH, Chaparro WA, Lizarazo JC (2016) Evaluation of single layer hafnium nitride coated tool for metal cutting. MRS Proc 1815:imrc2015.17. https://doi.org/10.1557/opl.2016.91
53. Navarro-Devia JH, Duque J, Aperador W, Amaya Hoyos CA (2016) Novel approach to evaluate the performance of [HfN/VN] n multilayer hard coatings deposited on cutting tools. In: XXV International Materials Research Congress 2016. CONACYT MRS-Mexico, Cancun
54. Oliver WC, Pharr GM (1992) An improved technique for determining hardness and elastic modulus using load and displacement sensing indentation experiments. J Mater Res 7:1564–1583. https://doi.org/10.1557/JMR.1992.1564
55. Baker SP, Liu J (2016) Nanoindentation techniques. In: Reference module in materials science and materials engineering. Elsevier
56. Caicedo JC, Zambrano OA, Aperador W (2018) Improvement of the useful life of the machining tool with the carbonitrides multilayer system. Int J Adv Manuf Technol 96:3263–3277. https://doi.org/10.1007/s00170-018-1826-z
57. Caicedo JC, Aperador W, Amaya C (2017) Determination of physical characteristic in vanadium carbon nitride coatings on machining tools. Int J Adv Manuf Technol 91:1227–1241. https://doi.org/10.1007/s00170-016-9835-2
58. Fox-Rabinovich G, Kovalev A, Aguirre MH, Yamamoto K, Veldhuis S, Gershman I, Rashkovskiy A, Endrino JL, Beake B, Dosbaeva G, Wainstein D, Yuan J, Bunting JW (2014) Evolution of self-organization in nano-structured PVD coatings under extreme tribological conditions. Appl Surf Sci 297:22–32. https://doi.org/10.1016/j.apsusc.2014.01.052
59. Yuan J, Dosbaeva J, Covelli D, Boyd J, Fox-Rabinovich GS, Veldhuis SC (2018) Study of tribofilms generation at different cutting speeds in dry machining hardened AISI T1 and AISI D2 steel. Proc Inst Mech Eng Part J J Eng Tribol 232:910–918. https://doi.org/10.1177/1350650117733921
60. Shihab SK, Khan ZA, Mohammad A, Siddiqueed AN (2014) RSM based study of cutting temperature during hard turning with

multilayer coated carbide insert. Procedia Mater Sci 6:1233–1242. https://doi.org/10.1016/j.mspro.2014.07.197
61. Rahim EA, Ibrahim MR, Rahim AA, Aziz S, Mohid Z (2015) Experimental investigation of minimum quantity lubrication (MQL) as a sustainable cooling technique. Procedia CIRP 26: 351–354. https://doi.org/10.1016/j.procir.2014.07.029
62. Abhang LB, Hameedullah M (2012) Selection of lubricant using combined multiple attribute decision- making method. Adv Prod Eng Manag 7:39
63. Brzezinka T, Rao J, Chowdhury M, Kohlscheen J, Fox Rabinovich G, Veldhuis S, Endrino J (2017) Hybrid Ti-MoS2 coatings for dry machining of aluminium alloys. Coatings 7:149. https://doi.org/10.3390/coatings7090149
64. Fox-Rabinovich G, Dasch JM, Wagg T, Yamamoto K, Veldhuis S, Dosbaeva GK, Tauhiduzzaman M (2011) Cutting performance of different coatings during minimum quantity lubrication drilling of aluminum silicon B319 cast alloy. Surf Coatings Technol 205: 4107–4116. https://doi.org/10.1016/j.surfcoat.2011.03.006
65. Kalpakjian S, Schmid SR (2014) Machining processes: turning and hole making. In: Manufacturing engineering and technology, 7th ed. Prentice Hall, Prentice Hall, pp 625–667
66. Kishore DSC, Rao KP, Mahamani A (2014) Investigation of cutting force, surface roughness and flank wear in turning of in-situ Al6061-TiC metal matrix composite. Procedia Mater Sci 6:1040–1050. https://doi.org/10.1016/j.mspro.2014.07.175
67. Kalpakjian S, Schmid SR (2014) Surface roughness and measurement; friction, wear and lubrication. In: Manufacturing engineering and technology, 7th edn. Prentice Hall, New York, pp 963–984
68. ISO (1993) ISO3685:1993. **Tool-life testing with single-point turning tools**
69. Shalaby M, Veldhuis S (2018) New observations on high-speed machining of hardened AISI 4340 steel using alumina-based ceramic tools. J Manuf Mater Process 2:27. https://doi.org/10.3390/jmmp2020027
70. Das SR, Panda A, Dhupal D (2017) Experimental investigation of surface roughness, flank wear, chip morphology and cost estimation during machining of hardened AISI 4340 steel with coated carbide insert. Mech Adv Mater Mod Process 3(9). https://doi.org/10.1186/s40759-017-0025-1
71. Binder M, Klocke F, Doebbeler B (2017) Abrasive wear behavior under metal cutting conditions. Wear 376–377:165–171. https://doi.org/10.1016/j.wear.2017.01.065
72. Nuñez PJ, Luis CJ, González C, Sebastian MA (2002) Estudio Comparativo de la Rugosidad Geometrica Obtenible en Procesos de Torneado // Comparative study of geometric roughness obtained in turning processes. Inf tecnológica 13:111–117
73. Shalaby MA, El Hakim MA, Abdelhameed MM et al (2014) Wear mechanisms of several cutting tool materials in hard turning of high carbon–chromium tool steel. Tribol Int 70:148–154. https://doi.org/10.1016/j.triboint.2013.10.011
74. Barry J, Byrne G (2002) The mechanisms of chip formation in machining hardened steels. J Manuf Sci Eng 124:528. https://doi.org/10.1115/1.1455643
75. Shalaby MA, El Hakim MA, Veldhuis SC, Dosbaeva GK (2017) An investigation into the behavior of the cutting forces in precision turning. Int J Adv Manuf Technol 90:1605–1615. https://doi.org/10.1007/s00170-016-9465-8
76. Dosbaeva GK, El Hakim MA, Shalaby MA et al (2015) Cutting temperature effect on PCBN and CVD coated carbide tools in hard turning of D2 tool steel. Int J Refract Met Hard Mater 50:1–8. https://doi.org/10.1016/j.ijrmhm.2014.11.001
77. Kumar CS, Patel SK (2018) Effect of chip sliding velocity and temperature on the wear behaviour of PVD AlCrN and AlTiN coated mixed alumina cutting tools during turning of hardened steel. Surf Coatings Technol 334:509–525. https://doi.org/10.1016/j.surfcoat.2017.12.013
78. TechMiny (2017) Types of chips in metal cutting to provide good surface finish & more. http://techminy.com/types-of-chips-in-metal-cutting. Accessed 11 Jul 2018
79. Kalpakjian S, Schmid SR (2014) Fundaments of machining. In: Manufacturing engineering and technology, 7th edn. Prentice Hall, New York, pp 566–599
80. Trent EM, Wright PK (2000) The essential features of metal cutting. In: Butterworth-Heinemann (ed) Metal cutting, 4th ed. Elsevier, pp 21–55
81. Paiva JM, Shalaby MAM, Chowdhury M, Shuster L, Chertovskikh S, Covelli D, Junior EL, Stolf P, Elfizy A, Bork CAS, Fox-Rabinovich G, Veldhuis SC (2017) Tribological and wear performance of carbide tools with TiB2 PVD coating under varying machining conditions of TiAl6V4 aerospace alloy. Coatings 7:187. https://doi.org/10.3390/coatings7110187
82. El Hakim MA, Abad MD, Abdelhameed MM et al (2011) Wear behavior of some cutting tool materials in hard turning of HSS. Tribol Int 44:1174–1181. https://doi.org/10.1016/j.triboint.2011.05.018
83. Kalpakjian S, Schmid SR (2014) Quality assurance, testing, and inspection. In: Manufacturing engineering and technology, 7th edn. Prentice Hall, New York, pp 1030–1056
84. Shi Y, Yang B, Liaw P (2017) Corrosion-resistant high-entropy alloys: a review. Metals (Basel) 7:43. https://doi.org/10.3390/met7020043
85. Askeland DR, Fulay PP, Wright WJ (2011) The science and engineering of materials, 6th ed. International Thomson, Stamford
86. Kajdas C, Harvey SSK, Wilusz E (1990) Encyclopedia of tribology, 1st ed. Elsevier, Amsterdam
87. Yuan J, Yamamoto K, Covelli D, Tauhiduzzaman M, Arif T, Gershman IS, Veldhuis SC, Fox-Rabinovich GS (2016) Tribofilms control in adaptive TiAlCrSiYN/TiAlCrN multilayer PVD coating by accelerating the initial machining conditions. Surf Coatings Technol 294:54–61. https://doi.org/10.1016/j.surfcoat.2016.02.041
88. Smith GT (2008) 7.7 tool wear and life. In: Cutting tool technology: industrial handbook. Springer London, London, pp 330–342
89. Chowdhury MSI, Chowdhury S, Yamamoto K, Beake BD, Bose B, Elfizy A, Cavelli D, Dosbaeva G, Aramesh M, Fox-Rabinovich GS, Veldhuis SC (2017) Wear behaviour of coated carbide tools during machining of Ti6Al4V aerospace alloy associated with strong built up edge formation. Surf Coatings Technol 313:319–327. https://doi.org/10.1016/j.surfcoat.2017.01.115
90. Fox-Rabinovich G, Weatherly GC, Kovalev A (2004) Tribology and the design of surface-engineered materials for cutting tool applications. In: Totten G, Xie L, Funatani K (eds) Modeling and simulation for material selection and mechanical design. Marcel Dekker, Inc., New York, USA
91. Fox-Rabinovich G, Gershman I, Hakim M, Shalaby M, Krzanowski J, Veldhuis S (2014) Tribofilm formation as a result of complex interaction at the tool/chip Interface during cutting. Lubricants 2:113–123. https://doi.org/10.3390/lubricants2030113